Title

A new brominated chalcone derivative suppresses the growth of gastric cancer cells in vitro and in vivo involving ROS mediated up-regulation of DR5 and 4 expression and apoptosis

Journal

Toxicology and Applied Pharmacology, 309

ISSN

0041-008X

Authors

Zhang, Saiyang
Li, Tingyu
Zhang, Yanbing
et al.

Publication Date

2016-10-01

DOI

10.1016/j.taap.2016.08.023

Peer reviewed

HHS Public Access

Author manuscript

Toxicol Appl Pharmacol. Author manuscript; available in PMC 2017 July 12.

Published in final edited form as:

Toxicol Appl Pharmacol. 2016 October 15; 309: 77–86. doi:10.1016/j.taap.2016.08.023.

A new brominated chalcone derivative suppresses the growth of gastric cancer cells in vitro and in vivo involving ROS mediated up-regulation of DR5 and 4 expression and apoptosis

Saiyang Zhang[a,1], **Tingyu Li**[a,1], **Yanbing Zhang**[a], **Hongde Xu**[a], **Yongchun Li**[a], **Xiaolin Zi**[b,c,d], **Haiyang Yu**[e], **Jinfeng Li**[f], **Cheng-Yun Jin**[a,*], and **Hong-Min Liu**[a,*]

[a]School of Pharmaceutical Sciences, Key Laboratory of State Ministry of Education, Key Laboratory of Henan province for Drug Quality Control and Evaluation, Collaborative Innovation Center of New Drug Research and Safety Evaluation, Zhengzhou University, 100 Kexue Avenue, Zhengzhou, Henan 450001, China

[b]Department of Urology, University of California, Irvine, Orange, USA

[c]Department of Pharmacology, University of California, Irvine, Orange, USA

[d]Department of Pharmaceutical Sciences, University of California, Irvine, Orange, USA

[e]Tianjin State Key Laboratory of Modern Chinese Medicine, Tianjin Key Laboratory of TCM Chemistry and Analysis, Institute of Traditional Chinese Medicine, Tianjin University of Traditional Chinese Medicine, 312 Anshanxi Road, Nankai District, Tianjin 300193, China

[f]Kidney Transplantation, The First Affiliated Hospital of Zhengzhou University, No. 1 Jianshe Road, Erqi District, Zhengzhou, Henan 450001, China

Abstract

A new series of 20 brominated chalcone derivatives were designed, synthesized, and investigated for their effects against the growth of four cancer cell lines (EC109, SKNSH, HepG2, MGC803). Among them, compound 19 which given chemical name of H72, was the most potent one on gastric cancer cell lines (i.e. MGC803, HGC27, SGC7901) with IC_{50s} ranged from 3.57 to 5.61 μM. H72 exhibited less cytotoxicity to non-malignant gastric epithelial cells GES-1. H72 treatment of MGC803 and HGC27 induced generation of reactive oxygen species (ROS) leading to activation of caspase 9/3 cascade and mitochondria mediated apoptosis. H72 also up-regulated the expression of DR5, DR4 and Bim_{EL}, and down-regulated the expression of Bid, Bcl-xL, and XIAP. *N*-acetyl cysteine (NAC), a ROS scavenger completely blocked these effects of H72 in MGC803 cells. Intraperitoneal administration of H72 significantly inhibited the growth of MGC803 cells in vivo in a xenograft mouse model without observed toxicity. These results

*Corresponding authors. cyjin@zzu.edu.cn (C.-Y. Jin), liuhm@zzu.edu.cn (H.-M. Liu).

[1]These authors contributed equally to this work.

Conflict of interest

The authors declare no competing or financial interests.

Transparency document

The Transparency document associated with this article can be found, in online version.

indicated that H72 is a lead brominated chalcone derivate and deserves further investigation for prevention and treatment of gastric cancer.

Keywords

Brominated chalcone; Apoptosis; Gastric cancer cells; ROS

1. Introduction

Gastric cancer is the fourth leading cause of global cancer mortality (Jemal et al., 2011; Siegel et al., 2014) and remains one of the most deadly malignant tumors among Asians (Rahman et al., 2014). Chemotherapy is an important therapeutic approach in the treatment of advanced gastric cancer, but its clinical applications are limited because of severe side effects (Qiu and Xu, 2013). Therefore, the development of a safe and more effective strategy for the treatment of gastric cancer is urgently needed.

The process of apoptosis includes the extrinsic and the intrinsic pathway (Cotter, 2009). The extrinsic pathway involves TRAIL binding to its receptors like DR4 and DR5. Death receptors form trimers rapidly and interact with FADD and transmit the apoptotic signals through activating caspase cascade which gives rise to apoptosis eventually (Liu et al., 2015). The intrinsic apoptosis pathway, also known as the mitochondrial or Bcl2 regulated apoptosis pathway, is regulated by the relative levels and activities of both pro- and anti-apoptotic members of the Bcl2 superfamily (Hutt, 2015). The intrinsic pathway is activated in response to intracellular stressors, induced by a litany of stimuli including DNA damage and growth factor withdrawal. These stress signals ultimately trigger that mitochondrial membrane (OMM) undergoes permeabilization, generally as a result of the activation of certain pro-apoptotic BCL-2 family members and some caspase family members and occurrence of apoptosis. (Wu and Bratton, 2013).

Chalcone is one of the major classes of naturally occurring compounds. Chalcone and its derivatives have generated great interest in medicinal chemistry, displaying a wide range of important pharmacological activities (Mahapatra et al., 2015). Millepachine, a novel chalcone, activates ROS-mitochondria mediated apoptotic pathway in human hepatocarcinoma cells in vitro and in vivo (Wu et al., 2013). In our previous study, combination therapy of naringenin chalcone and TRAIL reduced the clonogenic capacity, and surviving clones could be re-sensitized in human lung cancer A549 cells via up-regulating the expression of death receptor 5 (Jin et al., 2011). These observations suggested that naturally-occurring chalcone can be further optimized through synthesis of their derivatives as new anti-cancer agents to effectively treat certain cancers. Brominated substitution on ring A occurs relatively infrequently. The combination of brominated substitution with methoxy substituent on ring A has never been reported. Therefore, a series of brominated chalcone derivatives were rationally designed and their antitumor activities evaluated in this study.

Among them, H72 exhibited the strongest cytotoxic effect against gastric cancer cell lines via induction of ROS and mitochondria mediated apoptosis. In addition, H72 increased the

expression of DR4 and DR5, and Bim_{EL}, and decreased the expression of Bid, Bcl-xL, and XIAP. Furthermore, H72 demonstrated its strong in vivo anti-tumor activity in a xenograft model of MGC803 gastric cancer cells.

2. Materials and methods

2.1. Reagents

Fetal bovine serum (FBS), RPMI-1640, and penicillin–streptomycin were purchased from HyClone (Victoria, Australia). 3-(4,5-dimethyl-thiazol-2-yl)-2,5-diphenyltetra-zolium bromide (MTT), *N*-acetyl-L-cysteine (NAC) and JC-1 fluorescent dye (Sigma-Aldrich, St Louis, MO), z-VAD-fmk (Selleck, Texas, Houston), FITC/Annexin V Apoptosis Detection Kit (BestBio, Shanghai, China). 2,7-Dichlorodihydrofluorescein diacetate (DCFH-DA) was purchased from Beyotime Biotechnology (Shanghai, China). Antibodies specific for β-actin (sc-1615, goat, 1:1000), Bim_{EL} (sc-11425, rabbit, 1:1000), Bax (sc-493, rabbit, 1:1000), Bid (sc-11423, rabbit, 1:1000), caspase-3 (sc-7272, rabbit, 1:1000), caspase-9 (sc-7885, rabbit, 1:800), Cytochrome *c* (sc-7159, rabbit, 1:1000) and poly (ADP-ribose) polymerase-1 (PARP-1) (sc-7150, rabbit, 1:1000) were obtained from Santa Cruz Biotechnology (Santa Cruz, CA). Antibodies specific for Bcl-xL (#2764, rabbit, 1:1000) and XIAP (#14334, rabbit, 1:1000) were purchased from Cell Signaling Technology (Danvers, MA). The antibody specific for survivin (ab76424, rabbit, 1:2000) was purchased from Abcam (Cambridge, MA). Peroxidase-labeled anti-goat (1:5000), anti-rabbit (1:5000) and anti-mouse (1:5000) polyclonal immunoglobulins were purchased from Bioss (Shanghai, China). The enhanced chemiluminescence (ECL) kit was purchased from Thermo Fisher (Waltham, MA).

2.2. Chemosynthesis

The synthetic method to brominated chalcone derivatives **1–20** was shown in Fig. 1A. A mixture of substituted hydroxyacetophenone I (1.36 g, 1 eq), CH3I (1.85 g, 1.3 eq) and potassium carbonate (4.14 g, 3 eq) in acetone (12 ml) was stirred and refluxed for 4–6 h. The reaction system was evaporated to give a residue. Recrystallization from alcohol afforded the methoxy-substituted acetophenone II. Compound II (1.50 g, 1 eq) and bromosuccinimide (2.13 g, 1.2 eq) were dissolved in 40% H_2SO_4 (12 ml). The reaction mixture was stirred at 60 °C for 6 h. The reaction system was extracted with ethyl acetate (20 ml). The organic layer was dried over sodium sulfate, filtered, and evaporated. The residue was purified by silica gel column chromatography (hexane: ethyl acetate = 4:1) to give bromoacetophenone III. To the solution of compound III (1 eq) and aromatic aldehyde (1.2 eq) in ethanol, NaOH (2 eq) was added and stirred at RT for 6 h. The precipitate was filtered, washed with water, and dried to afford brominated chalcone derivatives IV.

The chemical structures of these brominated chalcones were identified using IR, ^{1}H NMR and ^{13}C NMR. And the spectrum data of the target compounds are given in the supplemental data.

2.3. Cell lines and cultures

EC109 (human esophagus cancer), MGC803 (human gastric cancer), SKNSH (human neuroblastoma), HepG2 (human hepatoma) cells, HGC27 (human gastric cancer), SGC7901 (human gastric cancer) and GES-1 (human gastric epithelial cell) were cultured at 37 °C in an atmosphere containing 5% CO_2, with RPMI-1640 medium supplemented with 10% heat-inactivated FBS, 100 U/ml penicillin and 0.1 mg ml^{-1} streptomycin.

2.4. Cell proliferation

Cells were seeded into a 96-well plate at a density of 4000 (100 μl) cells per well for 24 h, followed by treatment with compounds at indicated concentrations for additional 24 h. Next, 20 μl of 5 mg ml^{-1} MTT was added to the medium, and the cells were incubated for 4 h at 37 °C and 5% CO_2. After removing the culture medium, 150 μl of DMSO was added to dissolve the formazan crystals. The absorbance was recorded at 570 nm. The viability of vehicle control (0.1% DMSO) treated cells was set as 100%, and viabilities in the other groups was calculated by comparing the optical density reading with the control. The IC_{50} values were calculated using nonlinear regression analysis.

2.5. Apoptosis analysis

Cells were seeded at 1.5×10^5 cells per well in 6-well plates and cultured for 24 h. Next, the cells were exposed to different concentration of H72 for 24 h. After that, the cells were collected and washed with PBS twice, and then stained with fluorescein isothiocyanate (FITC)-conjugated Annexin V and then PI by following FITC Annexin-V/PI apoptosis kit instruction. Apoptotic cells were detected by flow cytometer. Annexin V+/PI- staining cells were counted as early apoptosis while Annexin V+/PI+ positive staining cells as late apoptotic/necrotic cells.

2.6. Measurement of ROS

The level of intracellular ROS was determined using DCFH-DA. Cells were seeded into a 6 well plate for 24 h. After that, cells were then subjected to H72 treatment for different periods of time. Following the treatment, cells were incubated with 20 mM DCFH-DA dissolved in cell-free medium at 37 °C for 30 min in the dark. After incubation, the cells were washed by PBS, trypsin, and collected by centrifugation, and washed three times again with PBS. The generation of intracellular ROS was assessed by fluorescence intensity (FL-1, 530 nm) using a flow cytometer.

2.7. Western blot analysis

Cells (1×10^6) were cultured in each 100 mm plate and treated with H72 or vehicle control for 24 h. After treatments, cells were collected and lysed with ice-cold lysis buffer (Beyotime, Shanghai, China). After centrifugation at 12,000 rpm min^{-1} for 30 min, protein concentrations of the lysates were determined by the micro-BCA protein assay kit. The total cellular protein extracts were boiled with 5 × loading buffer, separated by SDS-PAGE and transferred to nitrocellulose membrane. After blocking with 5% skimmed milk in PBS with 0.1% Tween-20 for 2 h, the membranes were incubated with appropriate antibodies overnight at 4 °C, followed by HRP conjugated anti-mouse, anti-goat or anti-rabbit

secondary antibodies. The detection of specific proteins was carried out with an ECL Western blotting kit according to the recommended procedure.

2.8. Measurement of mitochondrial membrane potential (MMP, ΔΨ)

Cells were seeded at 1.5×10^5 per well in 10% FBS RPMI-1640 into 6-well plates, and treated with H72 for 24 h. Then JC-1 (1 mg ml^{-1}) probe for measurement of MMP was added to incubate with an equal volume of cell suspension at 37 °C for 10 min and rinsed twice with PBS. The concentration of retained JC-1 dye was determined by a flow cytometer (In Hee et al., 2012).

2.9. Tumor xenograft growth assay in vivo

Twenty male nude mice (5 weeks old) were purchased from the Chinese Academy of Sciences (Beijing, China). All experiments were in accordance with the recommendations of the European Union regarding animal experimentation (Directive of the European Counsel 86/609/EC). Cells were digested and suspended in cold PBS at a density of 2.5×10^7 cells ml^{-1}. Cell suspension (200 μl) was subcutaneously injected into the nude mice on the right flank. Tumor growth was monitored by measurement of tumor volumes over time with calipers according to the formula, $V = 0.5 \times (\text{length} \times \text{width}^2)$. Body weights were also measured over time. The experiment was terminated at 21 days after tumor cell injection. Tumors were harvested and weighted.

2.10. Statistical analysis

The data are expressed as means ± SD. Statistical significance of the data was determined using a one-way analysis of variance (ANOVA) if not mentioned in the article. $p < 0.05$ was accepted as an indication of statistical significance.

3. Results

3.1. H72 significantly reduced the viabilities of human gastric cancer cell lines (MCG803, HGC27 and SGC7901) with minimal toxicity to non-malignant human gastric epithelial cells GES-1

Based on the screening results of twenty synthetic brominated chalcone derivatives for inhibiting the growth of cancer cell lines, the most potent brominated chalcone, H72, was prioritized to perform further experiment for evaluating its anti-cancer potential in gastric cancer (Fig. 1A and Table 1). Three gastric cancer cell lines (MGC803, HGC27 and SGC7901) and non-malignant human gastric epithelial cells (GES-1)were incubated with the indicated concentrations of H72 for 24 h, and then the effects of H72 on reducing cell viabilities were measured by an MTT assay (Cheol et al., 2012; Yu et al., 2012). As shown in Fig. 1B, following treatment with H72, the viability of the gastric cancer cells decreased in a concentration-dependent manner. MGC803 cells were the most sensitive to H72 treatment, causing 68.41% viability reduction in related to control treatment (Jeong et al., 2011). In contrast, non-malignant human gastric epithelial cells (GES-1) exhibited significantly less reduction of cell viability after H72 treatment (Fig. 1B). These results suggested that H72 has selective cytotoxicity against gastric cancer cells versus normal human gastric epithelial cells.

3.2. Effects of H72 on cell apoptosis in gastric cancer cells

We next examined whether the effect of H72 on reducing the viability of gastric cancer cells was the result of inducing apoptotic cell death. Fig. 2A showed that H72 treated cells exhibited typical morphological characteristics such as cell rounding and membrane blebbing (Veenman et al., 2010). As shown in Fig. 2B, treatment with H72 resulted in significant chromatin condensation, loss of nuclear construction, whereas these features were not observed in untreated cells.

We also quantitatively evaluated percentage of early and late apoptotic populations in H72 treated MGC803 and HGC27 cells using flow cytometry analysis of Annexin V and PI stained cells. Fig. 2B showed that H72 treatment increased the number of Annexin V positive staining cells in a concentration-dependent manner from 14.7% to 92.33% in MGC803 and 5.3% to 84.6% in HGC27 cells, whereas control treatment only resulted in 0.03% and 3.4% Annexin V positive staining cells, respectively. (Shang et al., 2008; Han et al., 2013).

3.3. H72-induced apoptosis involves the modulation of Bcl-2 and IAP family proteins, up-regulation of DR4 and 5, attenuation of MMP (ΔΨ), and release of cytochrome c in gastric cancer cells

The role of the Bcl-2 and the inhibitor of apoptosis protein (IAP) family proteins were determined by western blotting analysis to explore the possible mechanisms involved in H72-induced apoptosis in MGC803 cells (Han et al., 2013; Li et al., 2014). As shown in Fig. 3A. In comparison with the control cells, H72 treatment of MGC803 cells led to a significant increase in the protein levels of Bim_{EL}, DR4 and DR5 and a reduction in the protein levels of Bcl-xL, XIAP, and survivin, whereas the levels of pro-apoptotic Bax were not changed (Han et al., 2013). We also examined in detail the effects of H72 on Bid expression in MGC803 cells. Bid cleavage was assessed as a reduction in full-length Bid protein-the antibody used in the present study recognized only the full-length Bid molecule and not the cleavage product (Fig. 3A). Treatment with 6 μM of H72 for 24 h resulted in reduction of wild type Bid (indicating Bid cleavage) (Jin et al., 2009).

Mitochondria play an essential role in cell apoptosis pathway (Wang, 2001; Wang et al., 2013), and the mitochondria-dependent apoptotic pathway is regulated by the Bcl-2 family of pro- and anti-apoptotic proteins. To determine the role of the mitochondria in H72-induced apoptosis, we further evaluated the release of cytochrome *c* into the cytosol, as well as the change of MMP (ΔΨ). As shown in Fig. 3B, exposure of MGC803 cells to H72 induced a marked increase in the level of cytosolic cytochrome *c* released from the mitochondria. Furthermore, as shown in Fig. 3C, H72 significantly reduced MMP levels in a concentration-dependent manner in both MGC803 and HGC27 cells. These results suggested that H72 activated the mitochondria mediated apoptotic pathway in gastric cancer cells (Jeong et al., 2010).

3.4. Apoptosis induced by H72 in gastric cancer cells is partially caspase dependent

Caspases are known as key executioners of apoptosis through the cleavage of various cellular substrates (Matsuzaki et al., 2012). To further investigate whether H72-induced

apoptosis is associated with activation of the caspase cascade leading to proteolytic cleavage of poly(ADP-ribose) polymerases-1 (PARP-1) in MGC803 cells we assessed cleavage of caspases (−3 and −9) and PARP-1. As shown in Fig. 4A, Western blot analysis revealed that treatment of MGC803 cells with H72 down-regulated the levels of pro-caspase-3, pro-caspase-9 and pro-PARP-1 proteins accompanied by an increase in levels of cleaved caspase-3, 9 and PARP-1 proteins compared to the control treatment in MGC803 cells.

To further evaluate the significance of caspases activation in H72-induced apoptosis, MGC803 and HGC27 cells were pretreated with a caspase inhibitor z-VAD-fmk (100 μM) for 1 h, followed by 6 μM of H72 treatment for 24 h. As shown in Fig. 4B and C, Pretreatment with z-VAD-fmk partially attenuated H72-induced apoptosis from 82.1% to 39.6% (Fig. 4C). Taken together, these results suggest that H72-induced apoptosis is partially dependent of caspase activation in MGC803 cells.

3.5. H72-induced apoptosis is associated with ROS generation

The generation of intracellular ROS has been shown to be associated with mitochondria mediated induction of apoptosis in various cell types (Fulda and Debatin, 2006; Jeong et al., 2011). We therefore measured ROS production in MGC803 cells by flow cytometry analysis of cellular DCFH-DA fluorescence intensity. As shown in Fig. 5A, treatment of MGC803 cells with 6 μM of H72 resulted in a time-dependent increase of ROS generation. Next, to determine whether H72-induced ROS production was attributable to the growth inhibition and apoptosis induction, the cells were pretreatment with NAC for 1 h and co-incubated with H72 for an additional 24 h. Fig. 5B and C revealed that pretreatment of MGC803 and HCG27 cells with NAC almost completely blocked the H72-induced cell growth inhibition and apoptosis. In addition, Fig. 5D and E showed that NAC pretreatment reversed the effect of H72 on expression of Bcl-xL, Bid, XIAP, surviving, DR4 and DR5, as well as cleavage of caspase-3, caspase-9 and PARP-1 and alteration of MMP. These data suggested that the generation of ROS is required for the H72-induced apoptosis in gastric cancer cells.

3.6. H72 inhibits in vivo tumor growth in the xenograft nude mouse model of MGC803 cells

As shown in Fig. 6A, the growth rate of MGC803 xenograft tumors from mice which were treated with H72 was significant low than those from the vehicle control-treated mice. The mean of wet tumor weights in the H72 treated mice was about 60% less than that of the control treated mice (Fig. 6B) (Student's *t*-test; $P < 0.01$). There is no significant difference in mean body weights over time between control and H72 treated groups (Fig. 6C) (Student's *t*-test; $P < 0.05$). These results demonstrated the in vivo anti-tumor activity of H72 against gastric cancer cells.

4. Discussion

Chalcones represent key structural motif in the plethora of biologically active molecules 359 including synthetic and natural products (Singh et al., 2014). Synthesizing derivatives of Chalcones may be a good way for the development of more potent and efficient drugs for cancer. Synthesis of brominated derivatives is a common way to gain cellular potency of anti-cancer agents. The results that tested the anti-cancer activity of **1**–**20** on the four human

tumor cell lines showed that some of the compounds exhibited anti-proliferative activity at lower concentrations as compared with 5-FU as the positive control. Compared compounds **1**–**8** with **11**–**18**, we've found that compounds with 6′-OMe group on B ring is more potent than 3′-OMe ones. So we focused our discussion on compounds with 6′-OMe group (**9**–**20**). As for the groups on A ring, it's hard to figure out a clear rule to explain the effects, but we can still see some clues. Compounds with electron-withdrawing nitro group (**17**), methylsulfonyl group (**19**) on A ring generally have better activities on all four cell lines than others. Compounds with 4-halogen (**13**, **14**) on A ring exerted good activities on three cell lines except EC109, while compounds with 2-halogen (**15**, **16**) increase the activity on EC109 but decrease on the other three cell lines. Positions of methoxy groups on A rings has no significant effect, those compounds (**10**, **11**, **12**, **18**, **19**) all exerted good activity on four cell lines. In conclusion, we supposed that electronic effects on both rings may not play a major role on the antiproliferative activity of this kind of chalcone compounds. The space effect perhaps also plays a part.

The molecular mechanisms of H72 induced apoptosis were involved in up-regulation of Bim_{EL} expression and down-regulation of Bid, Bcl-xL, and XIAP expression, which resulted in a decrease of mitochondria potential and release of cytochrome *c* to activate caspase dependent apoptosis. Previous studies have also shown that other chalcone compounds caused similar molecular alterations in Bcl-2 family proteins and inhibitors of apoptotic protein leading to activate the mitochondria-mediated apoptosis in prostate cancer, bladder cancer, colon, lung, and breast cancers and sarcoma and others (Zi and Simoneau, 2005; Su et al., 2008; Gupta et al., 2013; Ji et al., 2013). Our results were consistent with these findings very well and confirmed a general mechanism for chalcone compounds activating the mitochondria-mediated apoptosis in cancers.

TNF-related apoptosis-inducing ligand (TRAIL) is secreted by most normal cells to induce apoptosis predominantly in tumor cells by binding to death receptors DR4 and DR5. Both Epirubicin and Oxaliplatin can enhance TRAIL-induced apoptosis in gastric cancer cells by regulating death receptors (Xu et al., 2009; Xu et al., 2011). We have shown here that H72 increased the expression of both DR4 and DR5 expression in gastric cancer cells. Therefore, it is possible that the increased expression of DR4 and DR5 by H72 may contribute to the selective toxicity of H72 toward gastric cancer cell lines (MGC803, HGC27, SGC7901) versus non-malignant human gastric epithelial cells (GES-1). Further experiments are in progress to determine whether H72 can serve as a novel TRAIL sensitizer to synergize TRAIL induced apoptosis in gastric cancer cells.

The mitochondrial electron transport machinery is thought to be a primary resource for ROS generation, which acts upstream of the mitochondria outer membrane permeabilization, cytochrome *c* release and caspase activation by certain apoptotic stimuli (Han et al., 2013; Atashi et al., 2015). Some studies indicate that anticancer effects of chalcone compounds are related to activation of oxidative stress response by hydroxyl substituted chalcones and cyclic chalcone analogues in mitochondria (Guzy et al., 2010). In addition, ROS has also shown to up-regulate the expression DR5 via the JNK-CHOP pathway (Trivedi et al., 2014; Chang et al., 2015). Therefore, ROS can trigger apoptosis through activation of both death receptors and the mitochondria mediated apoptotic pathway. In this study, we detected

down-regulation of the mitochondria membrane potential and release of cytochrome *c* from mitochondria to cytoplasm after treatment by indicated concentrations of H72. We have also shown that a ROS scavenger NAC co-treatment can completely reverse the effects of H72 on expression of DR4, DR5, Bid, Bcl-xL, and XIAP and on the loss of mitochondria potential, as well as on apoptosis. These results suggested that ROS generation plays a major role in H72 induced apoptosis in gastric cancer cells. Further experiments are therefore warranted to define the mechanism by which H72 induces ROS generation in cancer cells.

Our study have shown that H72, caused potent cytotoxic activity in vitro against gastric cancer cell lines with minimal effect on the growth of non-malignant human gastric epithelial cells. H72 reduces the viabilities of gastric cancer cell lines through induction of caspase- and ROS-dependent apoptosis. Importantly, H72 demonstrated in vivo anti-tumor activity in a xenograft model of gastric cancer MGC803 cells.

Supplementary Material

Refer to Web version on PubMed Central for supplementary material.

Acknowledgments

This work was supported by the National Natural Science Foundation of China (Project nos. 81430085 for Hong-Min Liu; Project nos. 81273393 for Yanbing Zhang; Project nos. 81272825 for Xiaolin Zi and Project nos. U1404821 for Cheng-Yun Jin) and the Scientific Innovation Talent Award from the Department of Education of Henan Province (no. 15HASTIT036 for Cheng-Yun Jin). We thank ZheSheng Chen and DongHua Yang from the College of Pharmacy and Health Sciences, St. Join's University for expert technical assistance.

References

Atashi F, Modarressi A, Pepper MS. The role of reactive oxygen species in mesenchymal stem cell adipogenic and osteogenic differentiation: a review. Stem Cells Dev. 2015; 24:1150–1163. [PubMed: 25603196]

Chang CC, Kuan CP, Lin JY, Lai JS, Ho TF. Tanshinone IIA facilitates TRAIL sensitization by up-regulating DR5 through the ROS-JNK-CHOP signaling axis in human ovarian carcinoma cell lines. Chem Res Toxicol. 2015; 28:1574–1583. [PubMed: 26203587]

Cheol P, Cheng-Yun J, Hye Jin H, Gi-Young K, Jung JH, Wun-Jae K, Young Hyun Y, Yung Hyun C. J7, a methyl jasmonate derivative, enhances TRAIL-mediated apoptosis through up-regulation of reactive oxygen species generation in human hepatoma HepG2 cells. Toxicol in Vitro. 2012; 26:86–93. [PubMed: 22079975]

Cotter TG. Apoptosis and cancer: the genesis of a research field. Nat Rev Cancer. 2009; 9:501–507. [PubMed: 19550425]

Fulda S, Debatin KM. Extrinsic versus intrinsic apoptosis pathways in anticancer chemotherapy. Oncogene. 2006; 25:4798–4811. [PubMed: 16892092]

Gupta SC, Francis SK, Nair MS, Mo YY, Aggarwal BB. Azadirone, a limonoid tetranortriterpene, induces death receptors and sensitizes human cancer cells to tumor necrosis factor-related apoptosis-inducing ligand (TRAIL) through a p53 protein-independent mechanism: evidence for the role of the ROS-ERK-CHOP-death receptor pathway. J Biol Chem. 2013; 288:32343–32356. [PubMed: 24078627]

Guzy J, Vaskova-Kubalkova J, Rozmer Z, Fodor K, Marekova M, Poskrobova M, Perjesi P. Activation of oxidative stress response by hydroxyl substituted chalcones and cyclic chalcone analogues in mitochondria. FEBS Lett. 2010; 584:567–570. [PubMed: 20004200]

Han MH, Park C, Jin CY, Kim GY, Chang YC, Moon SK, Kim WJ, Choi YH. Apoptosis induction of human bladder cancer cells by sanguinarine through reactive oxygen species-mediated up-regulation of early growth response gene-1. PLoS One. 2013; 8:e63425. [PubMed: 23717422]

Hutt KJ. The role of BH3-only proteins in apoptosis within the ovary. Reproduction. 2015; 149:R81–R89. [PubMed: 25336346]

In Hee K, Wook KS, Seong Hun K, Seung Ok L, Soo Teik L, Dae Ghon K, Jin LM, Woo Hyun P. Parthenolide-induced apoptosis of hepatic stellate cells and anti-fibrotic effects in an in vivo rat model. Exp Mol Med. 2012; 44:448–456. [PubMed: 22581380]

Jemal A, Bray F, Center MM, Ferlay J, Ward E, Forman D. Global cancer statistics. CA Cancer J Clin. 2011; 61:69–90. [PubMed: 21296855]

Jeong SY, Han MH, Jin CY, Kim GY, Choi BT, Nam TJ, Kim SK, Choi YH. Apoptosis induction of human leukemia cells by *Streptomyces* sp SY-103 metabolites through activation of caspase-3 and inactivation of Akt. Int J Mol Med. 2010; 25:31–40. [PubMed: 19956899]

Jeong JW, Jin CY, Park C, Su HH, Kim GY, Yong KJ, Lee JD, Yoo YH, Choi YH. Induction of apoptosis by cordycepin via reactive oxygen species generation in human leukemia cells. Toxicol in Vitro. 2011; 25:817–824. [PubMed: 21310227]

Ji T, Lin C, Krill LS, Eskander R, Guo Y, Zi X, Hoang BH. Flavokawain B, a kava chalcone, inhibits growth of human osteosarcoma cells through G2/M cell cycle arrest and apoptosis. Mol Cancer. 2013; 12:55. [PubMed: 23764122]

Jin CY, Park C, Moon SK, Kim GY, Kwon TK, Lee SJ, Kim WJ, Choi YH. Genistein sensitizes human hepatocellular carcinoma cells to TRAIL-mediated apoptosis by enhancing bid cleavage. Anti-Cancer Drugs. 2009; 20:713–722. [PubMed: 19617819]

Jin CY, Cheol P, Jin HH, Gi-Young K, Tae CB, Wun-Jae K, Hyun CY. Naringenin up-regulates the expression of death receptor 5 and enhances TRAIL-induced apoptosis in human lung cancer A549 cells. Mol Nutr Food Res. 2011; 55:300–309. [PubMed: 20669244]

Li JF, Huang RZ, Yao GY, Ye MY, Wang HS, Pan YM, Xiao JT. Synthesis and biological evaluation of novel aniline-derived asiatic acid derivatives as potential anticancer agents. Eur J Med Chem. 2014; 86:175–188. [PubMed: 25151580]

Liu X, Guo S, Liu X, Su L. Chaetocin induces endoplasmic reticulum stress response and leads to death receptor 5-dependent apoptosis in human non-small cell lung cancer cells. Apoptosis. 2015; 20:1499–1507. [PubMed: 26349783]

Mahapatra DK, Asati V, Bharti SK. Chalcones and their therapeutic targets for the management of diabetes: structural and pharmacological perspectives. Eur J Med Chem. 2015; 92c:839–865.

Matsuzaki J, Torigoe T, Hirohashi Y, Kamiguchi K, Tamura Y, Tsukahara T, Kubo T, Takahashi A, Nakazawa E, Saka E. ECRG4 is a negative regulator of caspase-8-mediated apoptosis in human T-leukemia cells. Carcinogenesis. 2012; 33:996–1003. [PubMed: 22411956]

Qiu MZ, Xu RH. The progress of targeted therapy in advanced gastric cancer. Biomark Res. 2013; 1:32. [PubMed: 24330856]

Rahman R, Asombang AW, Ibdah JA. Characteristics of gastric cancer in Asia. World J Gastroenterol. 2014; 20:4483–4490. [PubMed: 24782601]

Shang XJ, Yao G, Ge JP, Sun Y, Teng WH, Huang YF. Procyanidin induces apoptosis and necrosis of prostate cancer cell line PC-3 in a mitochondrion-dependent manner. J Androl. 2008; 30:122–126. [PubMed: 18974423]

Siegel R, Ma JM, Zou ZH, Jemal A. Cancer statistics, 2014. CA Cancer J Clin. 2014; 64:9–29. [PubMed: 24399786]

Singh P, Anand A, Kumar V. Recent developments in biological activities of chalcones: a mini review. Eur J Med Chem. 2014; 85:758–777. [PubMed: 25137491]

Su RY, Chi KH, Huang DY, Tai MH, Lin WW. 15-Deoxy-delta12,14-prostaglandin J2 up-regulates death receptor 5 gene expression in HCT116 cells: involvement of reactive oxygen species and C/EBP homologous transcription factor gene transcription. Mol Cancer Ther. 2008; 7:3429–3440. [PubMed: 18852146]

Trivedi R, Maurya R, Mishra DP. Medicarpin, a legume phytoalexin sensitizes myeloid leukemia cells to TRAIL-induced apoptosis through the induction of DR5 and activation of the ROS-JNK-CHOP pathway. Cell Death Dis. 2014; 5:e1465. [PubMed: 25321472]

Veenman L, Alten J, Linnemannstons K, Shandalov Y, Zeno S, Lakomek M, Gavish M, Kugler W. Potential involvement of F0F1-ATP(synth)ase and reactive oxygen species in apoptosis induction by the antineoplastic agent erucylphosphohomocholine in glioblastoma cell lines: a mechanism for induction of apoptosis via the 18 kDa mitochondrial translocator protein. Apoptosis. 2010; 15:753–768. [PubMed: 20107899]

Wang X. The expanding role of mitochondria in apoptosis. Genes Dev. 2001; 15:2922–2933. [PubMed: 11711427]

Wang X, Bai H, Zhang X, Liu J, Cao P, Liao N, Zhang W, Wang Z, Hai C. Inhibitory effect of oleanolic acid on hepatocellular carcinoma via ERK-p53-mediated cell cycle arrest and mitochondrial-dependent apoptosis. Carcinogenesis. 2013; 34:1323–1330. [PubMed: 23404993]

Wu CC, Bratton SB. Regulation of the intrinsic apoptosis pathway by reactive oxygen species. Antioxid Redox Signal. 2013; 19:546–558. [PubMed: 22978471]

Wu W, Ye H, Wan L, Han X, Wang G, Hu J, Tang M, Duan X, Fan Y, He S, Huang L, Pei H, Wang X, Li X, Xie C, Zhang R, Yuan Z, Mao Y, Wei Y, Chen L. Millepachine, a novel chalcone, induces G2/M arrest by inhibiting CDK1 activity and causing apoptosis via ROS-mitochondrial apoptotic pathway in human hepatocarcinoma cells in vitro and in vivo. Carcinogenesis. 2013; 34:1636–1643. [PubMed: 23471882]

Xu L, Qu X, Zhang Y, Hu X, Yang X, Hou K, Teng Y, Zhang J, Sada K, Liu Y. Oxaliplatin enhances TRAIL-induced apoptosis in gastric cancer cells by CBL-regulated death receptor redistribution in lipid rafts. FEBS Lett. 2009; 583:943–948. [PubMed: 19223002]

Xu L, Qu X, Luo Y, Zhang Y, Liu J, Qu J, Zhang L, Liu Y. Epirubicin enhances TRAIL-induced apoptosis in gastric cancer cells by promoting death receptor clustering in lipid rafts. Mol Med Rep. 2011; 4:407–411. [PubMed: 21468584]

Yu HY, Jin CY, Kim KS, Lee YC, Park SH, Kim GY, Kim WJ, Moon HI, Choi YH, Lee JH. Oleifolioside A mediates caspase-independent human cervical carcinoma HeLa cell apoptosis involving nuclear relocation of mitochondrial apoptogenic factors AIF and EndoG. J Agric Food Chem. 2012; 60:5400–5406. [PubMed: 22564025]

Zi X, Simoneau AR. Flavokawain , a novel chalcone from kava extract, induces apoptosis in bladder cancer cells by involvement of Bax protein-dependent and mitochondria-dependent apoptotic pathway and suppresses tumor growth in mice. Cancer Res. 2005; 65:3479–3486. [PubMed: 15833884]

Appendix A. Supplementary data

Supplementary data to this article can be found online at http://dx.doi.org/10.1016/j.taap.2016.08.023.

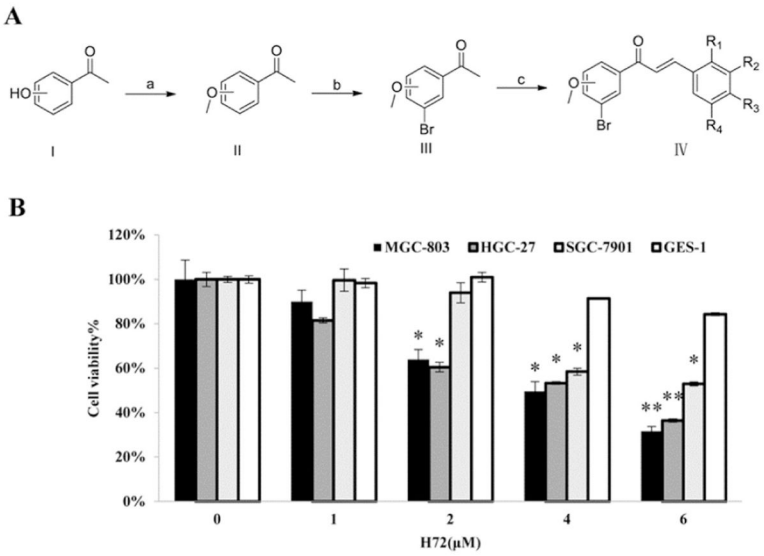

Fig. 1.

H72 is a lead compound for reducing viabilities of cancer cell lines. (A) Schematic presentation of the chemical synthesis route for brominated chalcone derivatives. Reagents: (a) MeI, K_2CO_3 acetone, reflux; (b) NBS, H_2SO_4, H_2O, 60 °C; (c) Aromatic aldehyde, NaOH, EtOH, r t. (B) The effect of H72 in reducing cell viabilities of gastric cancer cell lines (i.e. MGC803, HGC27, and SGC7901) and non-malignant gastric epithelial cells (GES-1) measured by MTT assay. The cells were treated with the indicated concentrations of H72 or culture medium for 24 h. The columns of each index have * $p < 0.05$, vs. untreated group; ** $p < 0.01$, vs. Untreated.

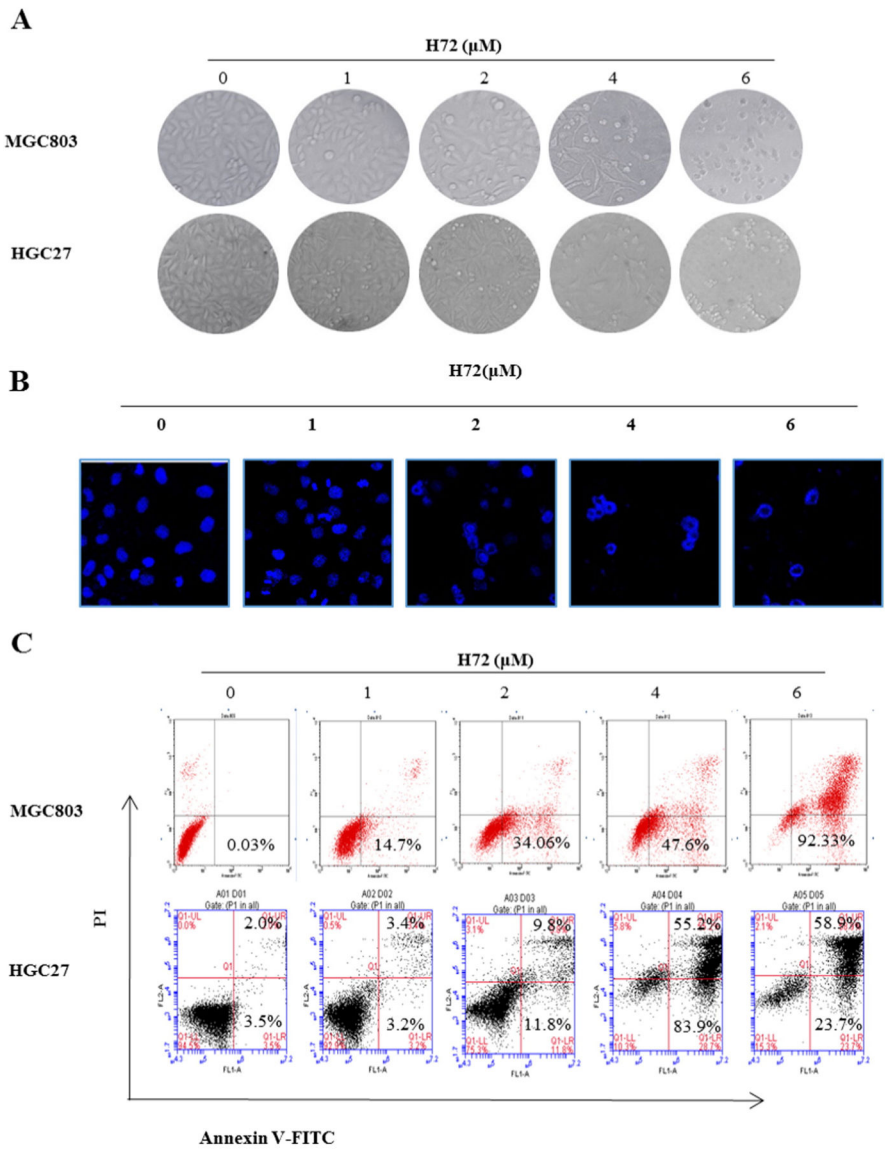

Fig. 2.

H72 induces apoptosis in gastric cancer cells. MGC803 and HGC27 cells were treated with vehicle control or varying concentrations of H72 for 24 h. (A) The morphological changes of cells were observed under an inverted microscope. (B) MGC803 cells were incubated with indicated concentrations of H72 for 24 h and then stained with DAPI. The stained nuclei were then observed under a fluorescent microscope (magnification, ×200). (C) Flow cytometric analysis of Annexin V/PI stained cells demonstrated a dose-dependent induction of apoptosis by H72.

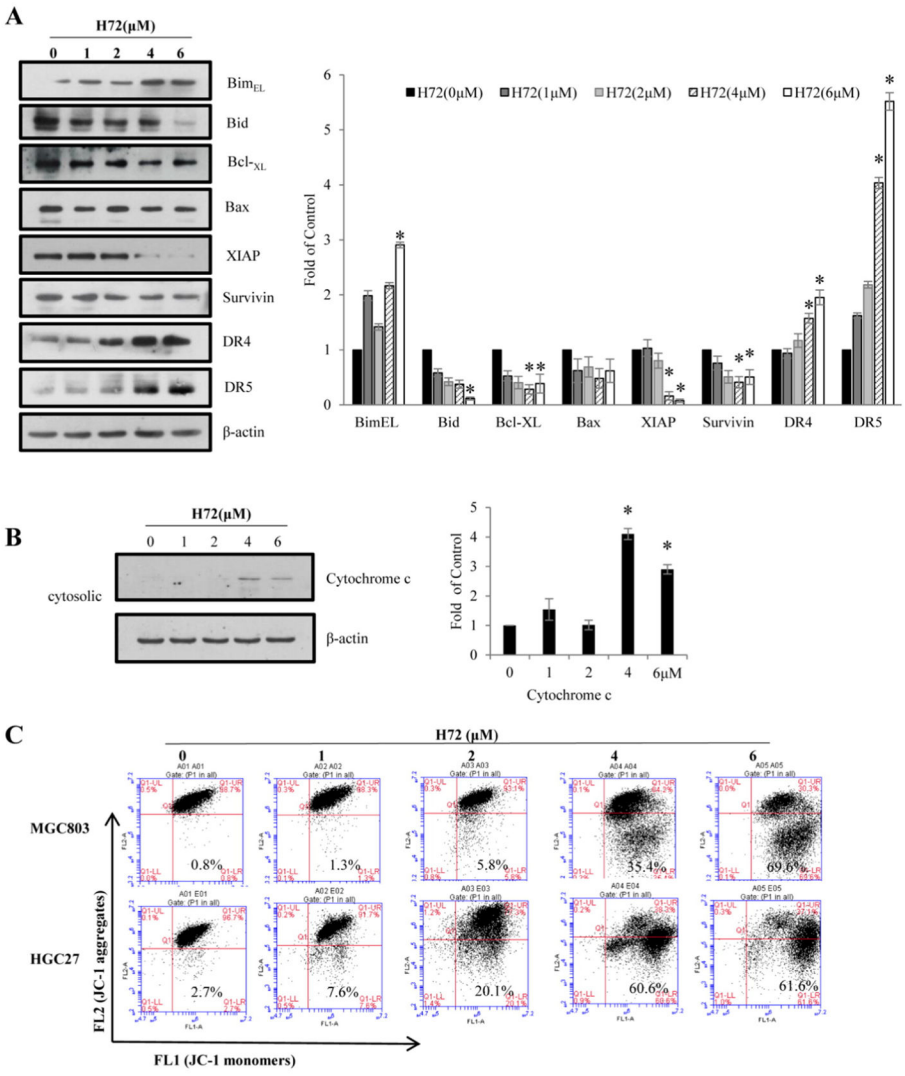

Fig. 3.

H72 induced apoptosis through modulation of Bcl-2 and IAP family proteins, attenuation of MMP (ΔΨ), and release of cytochrome *c* in MGC803 cells. (A) MGC803 Cells were treated with vehicle control or varying concentrations of H72 (0, 1, 2, 4 and 6 μM) for 24 h. The protein levels of Bax, Bim$_{EL}$, Bid, Bcl-xL, DR4, DR5, XIAP and Survivin were determined by Western blot assay. Density ratios of protein expression level after treatment by varying concentrations of H72 relative to control were shown in the histogram. (B) The effect of H72 on release of cytochrome *c* was measured by Western blot analysis of cytosolic protein in MGC803 cells. Density ratios of cytochrome *c* expression level after treatment by varying concentrations of H72 relative to control were shown in the histogram. (C) H72 decreased the membrane potential (ΔΨ) of the mitochondria. MGC803 and HGC27 cells were treated with vehicle control or varying concentrations of H72 (0, 1, 2, 4 and 6 μM) for 24 h. The mitochondria membrane potential was measured by JC-1 dye retention using flow cytometry. The columns of each index have * $p < 0.05$, vs. Untreated.

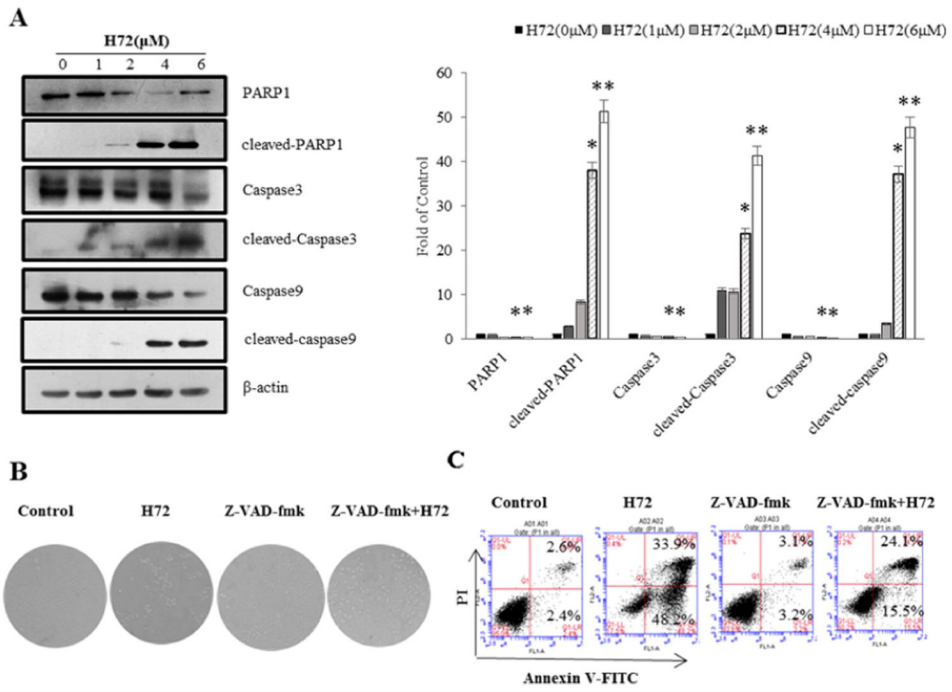

Fig. 4.

H72 activated caspase 3 and caspase 9. (A) Western blotting analysis showing the effects of H72 on the expression of cleaved-PARP1, cleaved-caspase3 and cleaved-caspase9. Density ratios of protein expression level after treatment by varying concentrations of H72 relative to control were shown in the histogram. (B) Representative photographs of morphological changes showed the effects of caspase inhibitor *Z*-VAD-fmk (100 μM) on H72 (6 μM)-treated MGC803 cells. (C) Flow cytometric analysis demonstrated the effect of Z-VAD-fmk(100 μM) on H72(6 μM)-induced cell apoptosis of MGC803 cells. The columns of each index have * $p < 0.05$, vs. Untreated; ** $p < 0.01$, vs. Untreated.

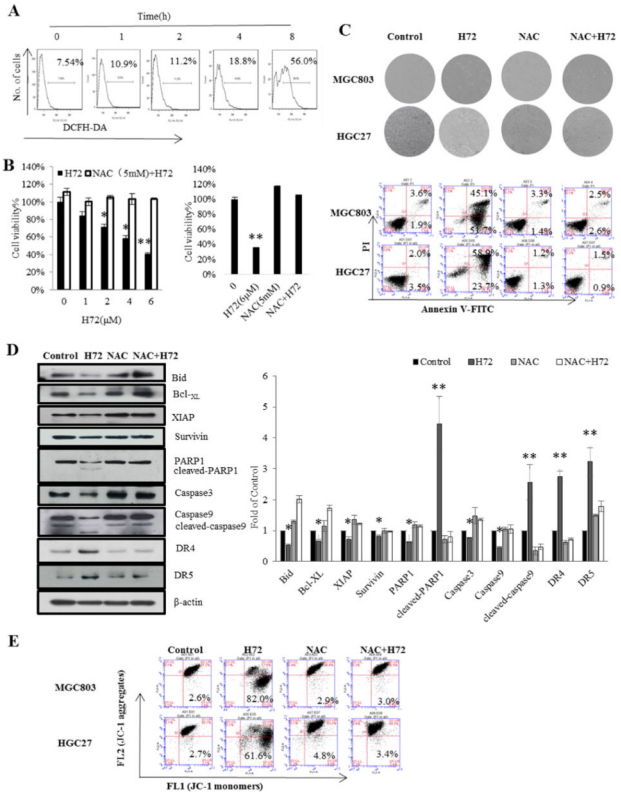

Fig. 5.

H72 induced ROS generation in gastric cancer cells. (A) Measurement of ROS. MGC803 cells were treated with 6 μM H72 for 0, 1, 2, 4, 8 h. The levels of ROS were measured by DCFH-DA with flow cytometry. (B) MTT assay demonstrates the effect of NAC (5 mM) on H72-induced cell death of MGC803 (left panel) and HGC27 cells (right panel). (C) Micrographs of morphological changes (upper panel) and Flow Cytometric analysis (lower panel) showed the effects of NAC (5 mM) on H72(6 μM)-induced cell apoptosis of MGC803 and HGC27 cells. (D) Western blot demonstrated the effect of NAC (5 mM) on H72-induced protein changes. Density ratios of protein expression level after treatment by H72(6 μM), NAC(5 mM) and H72 with pretreatment of NAC for 24 h relative to control were shown in the histogram. (E) Flow cytometric analysis showed the effects of NAC (5 mM) on H72 (6 μM)-induced loss of mitochondria membrane potential (ΔΨ) in MGC803 and HGC27 cells. The columns of each index have * $p < 0.05$, vs. Untreated; ** $p < 0.01$, vs. Untreated.

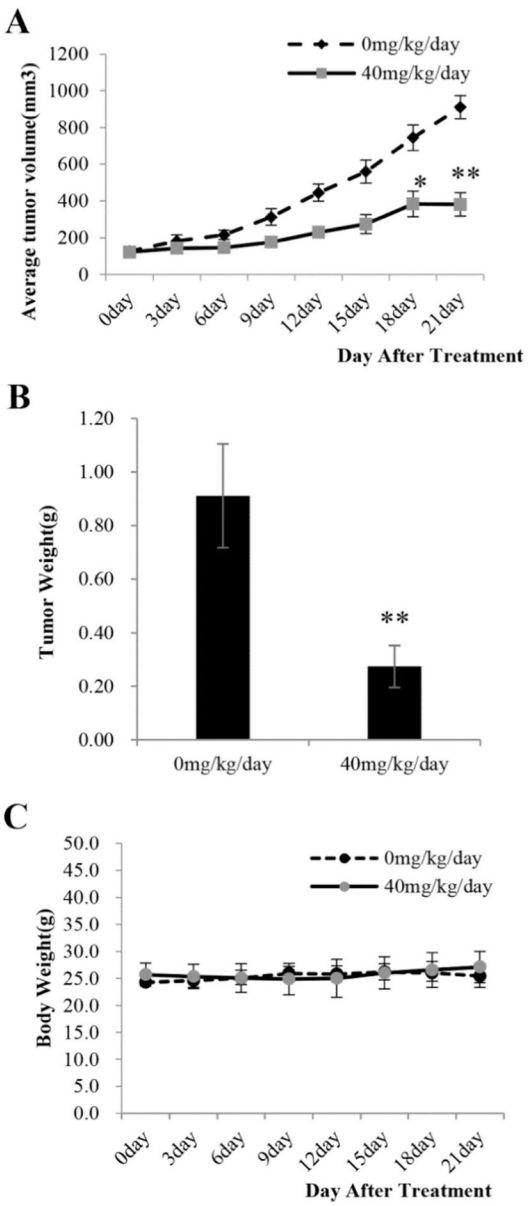

Fig. 6.

H72 inhibited tumor growth in vivo in the MGC803 xenograft model. (A–B) Statistical analyses demonstrated that the average volumes (A) and weights (B) of MGC803 xenograft tumors from vehicle control or H72-treated mice were significantly reduced. Treatments were initiated when the average size of the tumor reached 100 mm^3. The tested groups were treated with indicated dosage in 20 μl of DMSO of H72 daily and the control group received injection of DMSO alone. The mice ($n = 5$ per group) were treated for 21 days. (C) The body weight-time bar charts. The columns of each index have ** $p < 0.01$, vs. Untreated group.

Table 1

Chemical structures and IC50s of brominated chalcone derivatives (**1**–**20**).

Compound	IC50 (μM)			
	EC109	**SKNSH**	**HepG2**	**MGC803**
1 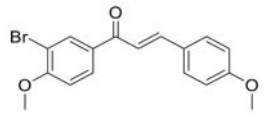	43.24	83.60	>100	>100
2 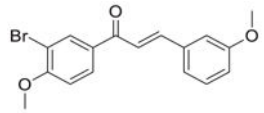	22.01	28.27	6.45	8.38
3 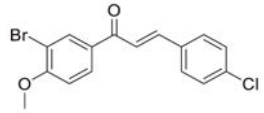	46.50	25.54	10.89	16.45
4 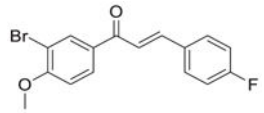	36.12	32.26	65.49	20.14
5 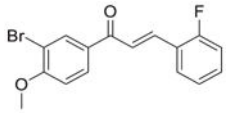	76.43	82.39	63.27	23.00
6 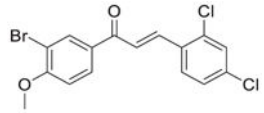	69.73	91.25	57.54	24.04
7 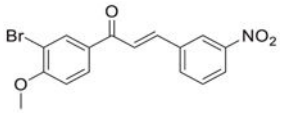	46.61	41.86	88.54	84.12

Compound	IC50 (μM)			
	EC109	SKNSH	HepG2	MGC803
8	>100	57.64	>100	>100
9	29.01	>100	47.53	18.41
10	13.56	7.22	13.32	5.41
5-FU	13.72	12.32	9.88	17.14
11	16.03	5.12	9.59	6.50
12	12.32	4.44	1.98	12.12
13	27.01	12.62	5.18	5.18
14	48.18	6.75	4.70	7.96

Compound	IC50 (μM)			
	EC109	SKNSH	HepG2	MGC803
15	18.99	12.07	99.50	70.61
16	14.67	18.70	19.98	11.02
17	8.11	4.19	10.03	8.76
18	10.09	4.91	13.39	12.00
19	5.61	8.25	6.39	3.57
20	14.65	7.13	5.60	6.16